



**UNIVERSITY OF LEEDS**

This is a repository copy of *Fretting–corrosion at the modular tapers interface: Inspection of standard ASTM F1875-98*.

White Rose Research Online URL for this paper:  
<http://eprints.whiterose.ac.uk/128760/>

Version: Accepted Version

---

**Article:**

Bingley, R, Martin, A, Manfredi, O et al. (8 more authors) (2018) Fretting–corrosion at the modular tapers interface: Inspection of standard ASTM F1875-98. Proceedings of the Institution of Mechanical Engineers, Part H: Journal of Engineering in Medicine, 232 (5). pp. 492-501. ISSN 0954-4119

<https://doi.org/10.1177/0954411918760958>

---

© IMechE 2018. This is an author produced version of a paper published as Bingley, R, et al. (2018) Fretting–corrosion at the modular tapers interface: Inspection of standard ASTM F1875-98. Proceedings of the Institution of Mechanical Engineers, Part H: Journal of Engineering in Medicine. Reprinted by permission of SAGE Publications.

**Reuse**

Items deposited in White Rose Research Online are protected by copyright, with all rights reserved unless indicated otherwise. They may be downloaded and/or printed for private study, or other acts as permitted by national copyright laws. The publisher or other rights holders may allow further reproduction and re-use of the full text version. This is indicated by the licence information on the White Rose Research Online record for the item.

**Takedown**

If you consider content in White Rose Research Online to be in breach of UK law, please notify us by emailing [eprints@whiterose.ac.uk](mailto:eprints@whiterose.ac.uk) including the URL of the record and the reason for the withdrawal request.



[eprints@whiterose.ac.uk](mailto:eprints@whiterose.ac.uk)  
<https://eprints.whiterose.ac.uk/>

## Fretting-Corrosion at the Modular Taper Interface: Inspection of standard ASTM F1875-98

Journal:	<i>Part H: Journal of Engineering in Medicine</i>
Manuscript ID	JOEIM-17-0151.R2
Manuscript Type:	Original article
Date Submitted by the Author:	24-Jan-2018
Complete List of Authors:	Bingley, Rachel; University of Leeds, Institute of Functional Surfaces (IFS), School of Mechanical Engineering. Martin, Alan; University of Sheffield, School of Mechanical Engineering Manfredi, Olivia; University of Sheffield, School of Mechanical Engineering Nejadhamzeeigilani, Mahdiyar; University of Leeds, School of Mechanical Engineering Oladokun, Abimbola; University of Leeds, Institute of Functional Surfaces (IFS), School of Mechanical Engineering. Beadling, Andrew; University of Leeds, Institute of Functional Surfaces (IFS), School of Mechanical Engineering. Siddiqui, Muhammad; University of Leeds, Institute of Functional Surfaces (IFS), School of Mechanical Engineering. Anderson, James; DePuy International Ltd Thompson, Jonathan; DePuy International Ltd Neville, Anne; University of Leeds, Institute of Functional Surfaces (IFS), School of Mechanical Engineering. Bryant, Michael; University of Leeds, Institute of Functional Surfaces (IFS), School of Mechanical Engineering.
Keywords:	fretting-corrosion, modular-taper, ASTM F1875-98, High Nitrogen Stainless Steel, CoCrMo
Abstract:	Interest in the degradation mechanisms at the modular-taper interfaces has been renewed due to increased reported cases of adverse reactions to metal debris and the appearance of wear and corrosion at the modular taper interfaces at revision. Over the past two decades a lot of research has been expended to understand the degradation mechanisms, with two primary implant loading procedures and orientations used consistently across the literature. ASTM F1875-98 is often used as a guide to understand and benchmark the tribocorrosion processes occurring within the modular-taper interface. This paper presents a comparison of the two methods outlined in ASTM F1875-98 as well as a critique of the standard considering the current paradigm in pre-clinical assessment of modular-tapers.

**Fretting-Corrosion at the Modular Taper Interface: Inspection of standard ASTM F1875-98**

Bingley, Rachel<sup>1</sup>, Martin, Alan<sup>2</sup>, Manfredi, Olivia<sup>2</sup>, Nejadhamzeeigilani, Mahdiyar<sup>1</sup>, Siddiqui, Sohail<sup>1</sup>, Oladokun, Abimbola<sup>1</sup>, Beadling, Andrew Robert<sup>1</sup>, Anderson, James<sup>3</sup>, Thompson, Jonathan<sup>3</sup>, Neville, Anne<sup>1</sup>, Bryant, Michael<sup>1</sup>

1. University of Leeds, Institute of Functional Surfaces (iFS), School of Mechanical Engineering, Leeds, UK
2. University of Sheffield, School of Mechanical Engineering, Sheffield, UK
3. DePuy International Ltd, Leeds, West Yorkshire, UK

For Peer Review

## Fretting-Corrosion at the Modular Taper Interface: Inspection of standard ASTM F1875-98

Bingley, Rachel<sup>1</sup>, Martin, Alan<sup>2</sup>, Manfredi, Olivia<sup>2</sup>, Nejadhamzeeigilani, Mahdiyar<sup>1</sup>, Siddiqui, Sohail<sup>1</sup>, Oladokun, Abimbola<sup>1</sup>, Beadling, Andrew Robert<sup>1</sup>, Anderson, James<sup>3</sup>, Thompson, Jonathan<sup>3</sup>, Neville, Anne<sup>1</sup>, Bryant, Michael\*<sup>1</sup>

1. University of Leeds, Institute of Functional Surfaces (iFS), School of Mechanical Engineering, Leeds, UK
2. University of Sheffield, School of Mechanical Engineering, Sheffield, UK
3. DePuy International Ltd, Leeds, West Yorkshire, UK

[\\*M.G.BRYANT@Leeds.ac.uk](mailto:M.G.BRYANT@Leeds.ac.uk)

### Abstract

Interest in the degradation mechanisms at the modular-taper interfaces has been renewed due to increased reported cases of adverse reactions to metal debris and the appearance of wear and corrosion at the modular taper interfaces at revision. Over the past two decades a lot of research has been expended to understand the degradation mechanisms, with two primary implant loading procedures and orientations used consistently across the literature. ASTM F1875-98 is often used as a guide to understand and benchmark the tribocorrosion processes occurring within the modular-taper interface. This paper presents a comparison of the two methods outlined in ASTM F1875-98 as well as a critique of the standard considering the current paradigm in pre-clinical assessment of modular-tapers.

**Keywords:** Fretting-Corrosion, Modular-Taper, ASTM F1875-98, High Nitrogen Stainless Steel, CoCrMo

### 1. Introduction

Interest in the performance of modular metal THR has recently been renewed due to the recent publicity associated with metal-on-metal bearings and the links to adverse reactions to metal debris (ARMD) [1]. Fretting-corrosion at the modular taper interface was first observed clinically at least 25 years ago [2]. Since then extensive effort has been made to understand the mechanisms at play at the modular taper interface and the interaction between implant and patient factors on clinical outcomes. The degradation of modular tapers is widely accepted as 'mechanically assisted' crevice corrosion as defined by Goldberg et al [3]. Whilst efforts have been made to optimise the taper interface in the 1990's, clinical incidence and awareness in the systemic effects of wear and corrosion at these interfaces has increased over the past 5 years [1].

One aspect that has been relatively unchanged is the testing and simulation techniques prescribed for the analysis of modular components. Uni-axial cyclic loading is often described and used extensively in the literature. ASTM F1875-98 [4] is a standard for quantifying the occurrence of fretting corrosion that occurs in the head-stem interface of a modular hip joint. ISO 7206-6 [5] also provides a method of assessment based on an upright stem orientation. Whilst the loading profiles are similar, mounting instructions differ when compared to the ASTM standard. Whilst these are not used to predict in-vivo performance, many researchers are using these methods to understand and interrogate mechanisms occurring in-vivo. Within ASTM F1875-98 two primary test methods, one

1  
2  
3 'upright' and one 'inverted', are provided. The inverted method additionally has the choice of two  
4 sub-methods, one of which includes electrochemical analysis. **A compromise between both**  
5 **scenarios has been adopted in literature, with the integration of electrochemical techniques within**  
6 **the upright 'physiologically relevant' sample orientation.**  
7

8 The mechanical loading profile is fundamentally the same for both orientations. However, the use of  
9 the inverted test method is not well documented in the literature. Differences such as fluid pressure,  
10 fluid ingress and retention of wear debris at the interface may affect the subsequent tribocorrosion  
11 processes. Some of these complicating differences likely occur *in-vivo* with actual components. This  
12 paper therefore aims to assess and compare the role of sample orientation on the degradation  
13 processes at the modular taper interface. The methods described in the ASTM F1875-98 standard  
14 were analysed with the inclusion of in-situ corrosion measurement and further surface analysis. The  
15 results and findings of this study will be further discussed and set in context with the current ASTM  
16 recommendations.  
17  
18

## 20 2. Methodology and Materials

### 23 2.1. Components and Apparatus

24 High nitrogen stainless steel C-Stem AMT femoral stems (12/14 taper, DePuy Synthes, UK) and Ø36  
25 mm M-Spec (DePuy Synthes, UK) high carbon CoCr femoral heads were tested in this study. The  
26 solution used for all electrochemical measurements was aerated 0.9% NaCl solution (pH ≈ 7.4) at 37  
27 °C, prepared using analytical grade reagents and deionised water. In each case 100 mL of fluid was  
28 used. Prior mounting of the head-stem structure within the test fixtures the femoral head was  
29 mounted onto the stem taper according to ASTM F1440 using specially design fixtures to ensure the  
30 taper and trunnion were kept concentric. The femoral head was assembled dry using a static load of  
31 2 kN.  
32  
33

34 The stem orientations investigated in this study are shown in Figure 1. Fixtures were designed to  
35 meet the standard but also allow for the same fixture to be used for both orientations. Stemmed  
36 components were orientated according to the ASTM F 1440 and fixed using a high edge retention  
37 metallographic resin to the cement indication markers given on the femoral stem. **In each case, the**  
38 **head – neck interface was immersed in 100 mL of 0.9 g/L NaCl.** The head force was actuated against  
39 a soft polymer ring to avoid depassivation of the femoral head surface. **All components were**  
40 **subjected to a cyclic sinusoidal load (300 – 3300 N) at 1 Hz for 1 million cycles using an E-10k fatigue**  
41 **machine (Instron, UK) to enable comparison of surfaces after each test.**  
42  
43  
44

45 Upon completion of fatigue testing the implants were carefully removed from the fixture and the  
46 components were separated. Head-taper pull off tests were conducted according to the ASTM  
47 F1440-98. The femoral stem-head combinations were mounted and secured between two parallel  
48 plates and secured to the machine test bed with the centre of the femoral head axial to the load cell.  
49 The actuator was brought down to the femoral head and a clamp fitted to facilitate a tensile pull off  
50 load. No additional load was applied to the femoral head. The actuator was then advanced in the  
51 tensile direction at a rate of 2 mm/s. Displacement was ceased when the test load reached 0 kN. The  
52 pull-off force was taken as the maximum measured force during separation.  
53  
54  
55  
56  
57  
58  
59  
60

## 2.2. Electrochemical Test Methods

In all cases, the fixed stem-head components acted as the working electrode (WE), facilitated via a conductive connection to the stem. The site of the connection and remaining interfaces were sealed using a silicone sealant to ensure they did not contribute to electrochemical and mass loss measurements. A combined silver-silver chloride (Ag/AgCl) reference electrode (RE) and platinum (Pt) counter electrode (CE) (Thermo-Scientific, UK) was used to complete the cell. All electrochemical measurements were conducted using an Autolab PGSTAT101 potentiostat (Metrohm, Netherlands) at an acquisition rate of 0.2 Hz.

Two electrochemical methodologies were employed in part reference to ASTM F1875-98:

- For tests where the taper interface was orientated in an upright configuration (Figure 1a), Open Circuit Potential (OCP) of the system was monitored continuously throughout cyclic loading. In this configuration, the potential difference between the test stem and the reference electrode was measured to provide a non-destructive semi-quantitative indication on the severity of corrosion at the taper interface. This is not prescribed by ASTM requirements but was included to facilitate comparison between loading configurations.
- For tests where the taper interface was orientated in an inverted configuration (Figure 1b), Zero Resistance Ammetry (ZRA) was employed as per the ASTM standard for the 'inverted' tests. In this configuration a high nitrogen stainless steel C-Stem AMT femoral stem acted as a second working electrode (WE2) in which the net anodic/cathodic current generated through corrosion and fretting-corrosion could be measured. The second femoral stem was immersed in the test to replicate the area of loaded stem concealed by the resin. The mixed potential of both femoral stems was also measured relative to a RE.

## 2.3. Surface and Solution Analysis

After testing, the taper interfaces were visually inspected and photographed. For surface form profiling a sub-micron accurate Coordinate Measuring Machine (CMM, Mitutoyo Legex 322, Japan) was used to map the surface using a  $\varnothing$  1 mm ruby and a point spacing of 0.2 mm. These points on the surface were used to generate a Cartesian coordinate cloud which was then imported into Sphere Profiler (RedLux, UK) software. Deviations from the original surface were analysed by excluding areas of known contact (which can be seen visually) and fitting the surface using conical taper geometric identities. By analysing damage noted on the surface, an estimate of the volume loss could be made.

Inductively Coupled-Mass Spectrometry (ICP-MS) was used to analyse elemental composition of the electrolytes post-test after 1 million cycles. 1 mL of test electrolyte was diluted to 10 mL with HNO<sub>3</sub> prior to analysis. Samples were centrifuged at 1000 RPM for 10 minutes to extract particulate from the electrolyte prior to dilution. Co59, Cr52, Mo96 and Fe57 isotopes were used to analyse test electrolytes.

Optical microscopy (OM) was used to analyse the taper surfaces post simulation. To enable access to the engaged portions of the taper-trunnion interface femoral heads were sectioned by wire erosion

along the axis perpendicular to the toggling motion. Surfaces were imaged at 5mm intervals long the taper.

### 3. Results

#### 3.1. Electrochemical measurements

Figure 2 shows the evolution of the open circuit and mixed potential over the duration of each test. Two distinct trends were observed; for the upright test (Figure 2a) an initial negative shift in the recorded potential was observed upon the initiation of fatigue, followed by ennoblement of the system to values more positive than noted before loading. For the inverted cell (Figure 2b) upon the application of cyclic loading a sustained decrease in OCP was observed. This remained lower than the original OCP recorded before the application of loading. For the inverted cell, at the point when load ceased, an ennoblement in the OCP was noted. This was not seen for the upright cell.

Figure 3 shows the ZRA net current measurements obtained from the inverted tests. Upon the application of cyclic loading an increase in the current was observed. This indicates an increase in current flow from WE1 to WE2, representing an increase in corrosion at the taper interface. In all cases a positive charge transfer was observed corresponding to a corrosive mass loss from the taper interfaces. Table 1 tabulates these and presents an estimate of the material lost due to corrosion (including static corrosion and mechanically induced corrosion) based on the assumptions that cobalt was the primary corrosion reactions (i.e.  $\text{Co} \rightarrow \text{Co}^{2+} + 2\text{e}^-$ ; molar mass = 58.9 g/mol, valence = 2).

Experiment	Charge transfer (Q)	Estimated corrosive mass loss (mg)
Inverted 1 (Fig 3a – red)	0.03	0.01
Inverted 2 (Fig 3b)	0.74	0.23
Inverted 3 (Fig 3a – black)	0.80	0.24

#### 3.2. ICP-MS

Figure 4 shows ICP-MS data for solution samples taken after upright (Figure 4a) and inverted (Figure 4b) testing (n = 3). Each measurement was conducted three times during each test and the results presented as an average  $\pm$  standard deviation. Differences were observed between the orientations with the inverted orientation demonstrating increased release of Co and Cr compared to the upright tests. No difference in Mo concentration was observed. An increase in Fe was noted in the upright cell compared to the inverted. In both cases a preferential release of Co was observed accounting for 50-70% of the total ions released. A correspondence between the release of ions in and alloy ratio was not observed.

### 3.3. Optical Photography

Figure 5 shows both surfaces of the taper interface after 1million cycles of fatigue loading in the upright cell. Little to no evidence of wear or corrosion was seen after the tests. Light abrasion of the female taper was seen in test 2, although not observed in the other tests.

Figure 6 shows the modular taper surfaces after 1 million cycles in the inverted cell. Evidence of wear and corrosion was observed in all cases. Corrosion deposits on both surfaces was seen. Imprinting of the male trunnion topography on the female taper surface was also observed, especially in 'test 2'.

### 3.4. CMM

Figure 7 shows the CMM profiles obtained for the upright tests. Some deviation away from the original surface was observed; in the region of 500 nm and within the accuracy of the machine. Such profiles were consistently observed in all upright test. This is also supported by optical images. Estimated volume loss is  $0.20\pm 0.048 \text{ mm}^3$ .

Figure 8 shows the CMM measurements for the inverted tests. Clear evidence of material loss was observed, with deviations from the original surface similar to those observed *in-vivo*. A Coup-contracoup appearance was observed, characteristic of a toggling action. Deviations in the region of 1.5 – 6  $\mu\text{m}$  were observed, with imprinting of the male trunnion threads on the taper surface visible. This is supported with digital photography and visual inspection. Estimated volume loss was  $0.84\pm 0.35 \text{ mm}^3$ .

Figure 9 shows the CMM plots for the male trunnion surface. Due to the nature of the fitting algorithms used, an accurate measurement of surface deviation is not possible due to the course nature of the threads. Qualitative assessment shows no visible loss of threads on either test.

### 3.1. Optical Light Microscopy

Figure 10 shows OM images taken across the length of the female taper surface. For the upright tests, the surface showed little deviation in surface appearance across the length of the taper with a typically machined surface evident. Towards the top end of the taper, evidence of corrosion was observed. For the inverted tests, evidence of damage was seen within the region of engagement. Evidence of corrosion was seen, along with imprinting of the trunnion thread surface onto the surface of female taper, as indicated by the white arrows. The extent of corrosive damage increase towards the top end of the taper.

## 4. Discussion

Fretting-corrosion, fretting-crevice corrosion and mechanically assisted crevice corrosion are terms interchangeably used to describe the processes occurring at the interface [1,9]. The use of passive metallic materials has been practiced extensively in the orthopaedic sector since the 1950s. However, when used in load-bearing aqueous environments, corrosion and wear are inevitable. This combination of mechanical and electrochemical factors enhances degradation of materials – better known as tribocorrosion [6]. This describes the co-existence and inseparable action of corrosion and

1  
2  
3 wear owing to abrasion of the native oxide film and exposure of the reactive bulk alloy. As a result,  
4 metallic ions and particles are generated, potentially resulting in local and systemic biological  
5 reactions. Whilst an initial body of work was conducted in this area in the 1990's by Goldberg and  
6 co-workers [3, 7-11], simulation methods and interrogation of the test standards remain unexplored.  
7

8 The results from this study further the current understanding by highlighting some key differences  
9 between methods prescribed by ASTM and ISO. Whilst some variables (e.g. durations and loading  
10 rates) differed from those described by the standard, this was done to ensure results were  
11 comparable between each test series. In summary;  
12

- 13 • Differences in outcomes based on component orientation were observed – a higher degree of  
14 material loss was observed using ASTM F 1875 method II.
- 15 • Inclusion of electrochemical, CMM and ICP-MS methods are vital if degradation mechanisms at  
16 the interface are going to be determined.
- 17 • Fretting-corrosion at the modular surface can occur in stainless steel – CoCrMo alloys systems; a  
18 lesser investigated system despite the high levels of implantation especially in the United  
19 Kingdom.  
20  
21

22 The tribocorrosion processes occurring at the modular taper interface are well studied. However,  
23 the investigation of stainless steel-CoCrMo combinations has not received much attention despite its  
24 use in UK and EU markets. Gilbert et al [12] presented a systematic study showing high nitrogen  
25 stainless steel (Orthinox 90™)-CoCrMo systems to be more susceptible to corrosion when assembled  
26 under wet and dry conditions when compared to all CoCrMo systems. Chaplin et al [13]  
27 demonstrated evidence of fretting and corrosion on retrieved Exeter stainless steel femoral stems.  
28 However when compared to the work presented by Gilbert and Goldberg [7] the extent of corrosion  
29 was not as great. Despite this study demonstrating the existence of wear and corrosion at the head-  
30 neck interface, reports of clinical revisions are low and high nitrogen stainless steel femoral stems  
31 with CoCrMo femoral heads remain the gold standard for cemented THR [14]. Extensive work has  
32 been carried out to identify the role of taper variables such as finish, angle, length etc. and the  
33 incidence of revision. Morlock et al. along with many other researchers [15-17] have presented data  
34 concerning the roles of taper engagement mechanisms and surface finish on the degradation of  
35 modular tapers.  
36  
37  
38  
39

40 Clear differences can be seen between the two different implant orientations suggested by ASTM F  
41 1875-98 with electrochemical, ICP-MS, digital photography and CMM measurements supporting  
42 this. Electrochemical measurements proved a useful tool in assessing the effects of implant  
43 orientation. A negative shift in potential was observed for both arrangements at the onset of cyclic  
44 loading. However, for Method II, a sustained cathodic excursion in OCP was observed in the inverted  
45 tests suggesting a sustained increased rate of corrosion. This is complemented by ZRA  
46 measurements which indicate a net anodic current exchange from the inverted system suggesting  
47 under these conditions, abrasion of the oxide layer is sustained resulting in an increase in corrosion  
48 during inverted cyclic loading. For Method I, an ennoblement in the potential for the upright  
49 arrangements was observed suggesting a decrease in oxide abrasion and subsequently metal ion  
50 release. Although Method I does not prescribe electrochemical measurement, the differences  
51 observed in this study demonstrate the need for such measurement methods. ICP-MS supported the  
52 electrochemical results. Where a sustained decrease in potential and subsequent increase in current  
53 was observed, an increase in the metallic ions found within the test lubricant was seen. Cobalt was  
54  
55  
56  
57  
58  
59  
60

1  
2  
3 found to be the dominant element (49% of upright ions and 74% of inverted ions) suggesting  
4 degradation was concentrated on the CoCrMo taper surface. The increased Co levels may arise to  
5 the formation of Cr<sub>2</sub>O<sub>3</sub> oxide phases within the interface retaining Cr within the interface similar to  
6 that observed at the stem-cement interface [18].  
7

8 A higher degree of material loss was observed in the inverted system supporting the electrochemical  
9 results. In both orientations regions of taper engagement could be visually observed. However  
10 transfer of the stem taper 'threads' was only observed on the inverted tests (Figure 6 and Figure 10).  
11 This transfer is consistent with clinical and other in-vitro observations [19-22]. **The role of surface  
12 topography and the underlying mechanisms of trunnion thread imprinting onto the CoCrMo female  
13 taper surfaces are still not fully understood. Pourzal et al. [17] recently investigated the role of  
14 surface topography on the degradation of CoCr/Ti alloy modular taper interfaces. For CoCr-CoCr  
15 systems an increase in thread height was associated with lower Goldberg damage scores whilst  
16 surface roughness had a dominant influence for CoCr/Ti alloy couples. It must be noted that the  
17 correlations reported by Pourzal et al. can only be applied for the material combinations and taper  
18 designs reported in this study. Further consideration must be taken before such concepts and  
19 findings are applied to other material combinations and taper designs. The manufacturing processes  
20 and the way in which the material responds to these processes will also vary between taper designs  
21 and manufacturers. It is reasonable to assume that the local interfacial metallurgy, chemistry and  
22 mechanical properties will be affected and as a result will impact on the evolution wear and  
23 corrosion [23-25]. Whilst consideration of the male taper topography is an important variable in  
24 modular taper design, the main driver behind the surface topography in modularity must not  
25 forgotten; to facilitate the use of different head materials. Although topography is one aspect of  
26 consideration, it is obvious that the taper machined surface is one variable in a fine balancing act  
27 contributing to the design of an optimum modular taper.**  
28  
29  
30  
31  
32  
33

34 Visual evidence of oxide formation within and at the interface was observed further strengthening  
35 the ratio of metallic elements found in the solution by ICP-MS. For the inverted tests (Method II),  
36 material loss was concentrated at either ends of the bore suggesting a coup-count-coup mechanism  
37 (i.e. rocking motion), consistent with *in-vitro* observations [16]. CMM analysis of the upright system  
38 demonstrated minimum deviation from the original surface. This again compliments  
39 electrochemical, solution chemistry analysis and visual assessment. In all cases, material loss from  
40 the trunnion was limited. Whilst material loss was predominantly from the CoCrMo surface (i.e.  
41 taper), ICP-MS indicated higher Fe ion release under Method I – we hypothesise that this occurred as  
42 a result of inability for crevice corrosion to occur within the taper interface.  
43  
44  
45

#### 46 Critique of ISO/ASTM Methodologies

47  
48 To fully understand the degradation a combined electrochemical, mechanical, surface and solution  
49 analytical approach must be taken if advances in modular-taper developments are to be made.  
50 Whilst many researchers utilise a combination of these methods, standards do not reflect this. The  
51 following aspects of the ISO and ASTM standards will be discussed:  
52

- 53 • Sample Orientation
- 54 • Electrochemical Evaluation
- 55 • Sample Loading
- 56
- 57
- 58
- 59
- 60

1  
2  
3 **Sample Orientation** - Whilst the mechanical loading is assumed to be the same in both  
4 configurations, fluid pressures at the interface and the rate at which fluid can penetrate will vary.  
5 Although the reasons for this are not fully understood at this time, it is hypothesised that fluid  
6 ingress is an important factor at the interface facilitating an increased rate of wear and corrosion.  
7 During in-vitro testing it may be the case that during the inverted position, fluid ingress will at a  
8 higher rate, electrochemically 'activating' areas of the interface that otherwise would be unexposed  
9 to the electrolyte and therefore not subject to corrosion processes. Higher rates of degradation will  
10 occur due to the synergistic nature of fretting-crevice corrosion when compared to the upright  
11 system in which liquid does not penetrate. Although this highlights an important aspect concerning  
12 the pre-clinical assessment of modular neck tapers it also raises questions as to the operating  
13 environment *in-vivo* (i.e. could a pressurisation exist due to the surrounding tissues).  
14

15 **Electrochemical Evaluation** – Although a debate around the correct electrochemical measurement  
16 technique for the long-term evaluation of implants continues between researchers, it can be agreed  
17 that such methods provide real-time data regarding the kinetics of the corrosion processes occurring  
18 at the interface. ASTM F 1875, the only standard to prescribe electrochemical methods, describes  
19 the use of three different electrochemical methods: open circuit potential, potentiostatic  
20 polarisation and zero-resistance ammeter measurements, each of which return slightly different  
21 measurements. Based on Method I, no electrochemical methods are described. This test method is  
22 similar to the one outlined by ISO 7206-6.  
23

24 **Sample Loading** – The effects of sample loading and rates also need to be considered when dealing  
25 with a tribocorrosion system. Whilst it is universally agreed that a simple sinusoidal loading does not  
26 replicate the physiological gait, it is used as a simplified loading profile. Mroczkowski [26] and  
27 Pantagorgio et al [19] demonstrated the important of load showing increasing load and torsional  
28 bending moments can have an antagonistic effect on the corrosion at the interface. Preuß et al [27]  
29 examined the role of bending moment and frictional torque on the rotational stability of modular  
30 tapers when mated with a Biolox Ceramic heads under static loading within a hip simulator. It was  
31 demonstrated that rotational stability was reduced after frictional rotation although no further  
32 analysis was completed. Despite the steps to better understand the role of other motions, work to  
33 quantify fretting-corrosion under complex biomechanical loading is still to be done. This includes  
34 analysis under standard gait, daily living and extreme conditions. Rates of loading also need to be  
35 considered – two different loading rates are given within the standard (Method 1: 10 Hz & Method  
36 II: 1 Hz). It is unknown if wear and corrosion processes at this interface can be scaled appropriately  
37 for different rates of loading. Whilst wear may be considered proportional to the number of loading  
38 cycles (assuming a typical Archard's type relationship) corrosion and its synergies will not as factors  
39 such as oxygen transportation and the exchange of fluid within the interface will be affected alerting  
40 subsequent rates of re-passivation [7].  
41  
42  
43  
44

## 45 5. Summary and Conclusions

46 The issue of modular taper corrosion is a current and future issue faced by industry and clinicians.  
47 However, until effective methods of simulation are developed, future technologies will suffer from  
48 the same underpinning flaw. Furthermore, considering the advances in modern hip simulations for  
49 the bearing surfaces, simulations for the modular taper still remain primitive, only considering 2D  
50 motions at most. It has been observed in this study and the current clinical situations that current  
51 test standards do not adequately replicate conditions observed in-vivo. Furthermore, depending on  
52 the test method employed, very different damage characteristics could be observed; replicated  
53 closer those seen in-vivo. This suggest that despite the large body of work completed in this area, a  
54 full appreciation of the environment is not evident. Based on the number of studies that have been  
55 published in this area care must be taken when interpreting results as these appear to be both  
56  
57  
58  
59  
60

1  
2  
3 implant and test system specific (i.e. loading orientation, load actuation). Focussed efforts are  
4 needed to develop generally accepted more complex, multi-axis mechanical simulations with in-situ  
5 and real time multi-modal sensing capabilities. Furthermore, clarity regarding the test orientation  
6 and the inclusion of in-situ electrochemical measurements in all tests where corrosion is dominant is  
7 required. This study has also highlighted the importance of fluid penetration and possible retention  
8 of debris within the fretting-contact in the degradation of modular-tapers. Whilst we have observed  
9 instances of fretting-corrosion at the interface of stainless steel – CoCrMo contacts, the clinical  
10 occurrence remains unclear.

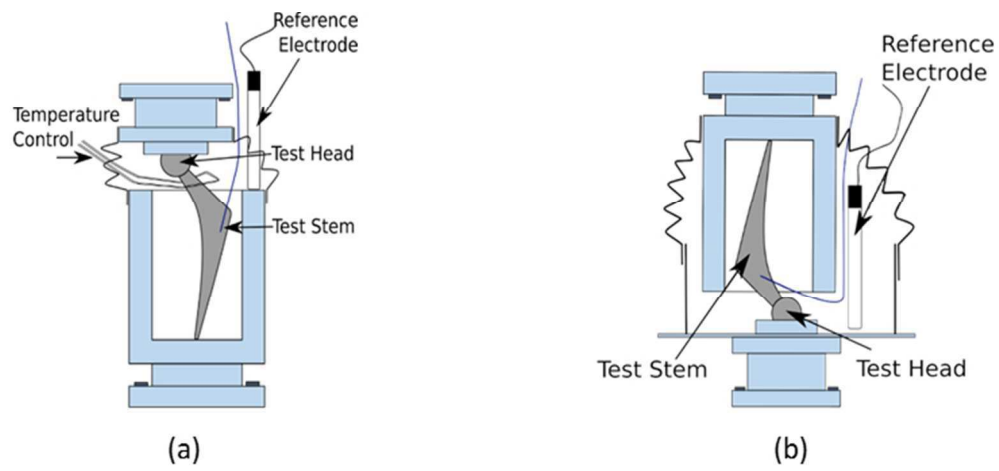
### 11 **Acknowledgements**

12 We would like to thank DePuy Synthes for donation of these components for evaluation.

### 13 **References**

- 14  
15  
16  
17 **1 Morlock, M.M.** The taper disaster - How could it happen? *HIP International*, 2015, **25**(4),  
18 339-346.  
19 **2 Collier, J., Surprenant, V., Jensen, R., Mayor, M. and Surprenant, S.** Corrosion between the  
20 components of modular femoral hip prostheses. *Journal of bone and joint surgery [Br]*, 1992, **74-B**,  
21 511-517.  
22 **3 Goldberg, J.R., Jacobs, J.J. and Gilbert, J.L.** In-vitro fretting corrosion testing of modular hip  
23 implants. *Transactions of the Annual Meeting of the Society for Biomaterials in conjunction with the*  
24 *International Biomaterials Symposium*, p. 8651996).  
25 **4 International, A.** Standard Practice for Fretting Corrosion Testing of Modular Implant  
26 Interfaces: Hip Femoral Head-Bore and Cone Taper Interface. . (ASTM International USA, 1998).  
27 **5 Standards, B.** BSI ISO 7206-6:2013 Implants for surgery — Partial and total hip joint  
28 prostheses. Part 6: Endurance properties testing and performance requirements of neck region of  
29 stemmed femoral components. (BSI Standards UK, 2013).  
30 **6 Yan, Y., Neville, A., Dowson, D. and Williams, S.** Tribocorrosion in implants: assessing high  
31 carbon and low carbon CoCrMo alloys by in situ electrochemical measurements. *Tribology*  
32 *International*, 2006, **39**(12), 1509-1517.  
33 **7 Goldberg, L. and Gilbert, J.** In Vitro Corrosion Testing of Modular Hip Tapers. *J Biomed Mater*  
34 *Res Part B*, 2003, **64B**, 79-93.  
35 **8 Goldberg, J.R., Buckley, C.A., Jacobs, J.J. and Gilbert, J.L.** Corrosion testing of modular hip  
36 implants. *ASTM Special Technical Publication*, 1997, **1301**, 157-176.  
37 **9 Gilbert, J.L., Buckley, C.A., Jacobs, J.J., Bertin, K.C. and Zernich, M.R.** Intergranular  
38 corrosion-fatigue failure of cobalt-alloy femoral stems. A failure analysis of two implants. *Journal of*  
39 *Bone and Joint Surgery - Series A*, 1994, **76**(1), 110-115.  
40 **10 Brown, S.A., Flemming, C.A.C., Kawalec, J.S., Placko, H.E., Vassaux, C., Merritt, K., Payer,**  
41 **J.H. and Kraay, M.J.** Fretting corrosion accelerates crevice corrosion of modular hip tapers. *Journal*  
42 *of applied biomaterials*, 1995, **6**(1), 19-26.  
43 **11 Boggan, R.S., Lemons, J.E. and Rigney, E.D.** Clinical and laboratory investigations of fretting  
44 and corrosion of a three-component modular femoral stem design. *Journal of long-term effects of*  
45 *medical implants*, 1994, **4**(4), 177-191.  
46 **12 Gilbert, J.L., Mehta, M. and Pinder, B.** Fretting crevice corrosion of stainless steel stem–  
47 CoCr femoral head connections: Comparisons of materials, initial moisture, and offset length.  
48 *Journal of Biomedical Materials Research Part B: Applied Biomaterials*, 2009, **88B**(1), 162-173.  
49 **13 Chaplin, R.P., Lee, A.J. and Hooper, R.M.** Assessment of wear on the cones of modular  
50 stainless steel Exeter hip stems. *J Mater Sci Mater Med*, 2004, **15**(9), 977-990.  
51 **14 National Joint Registry for England, Wales and Northern Ireland 11th Annual Report 2014.**  
52 [http://www.njrcentre.org.uk/njrcentre/NewsandEvents/NJR11thAnnualReport/tabid/363/Default.as](http://www.njrcentre.org.uk/njrcentre/NewsandEvents/NJR11thAnnualReport/tabid/363/Default.aspx)  
53 [px](http://www.njrcentre.org.uk/njrcentre/NewsandEvents/NJR11thAnnualReport/tabid/363/Default.aspx), 2015).  
54  
55  
56  
57  
58  
59  
60

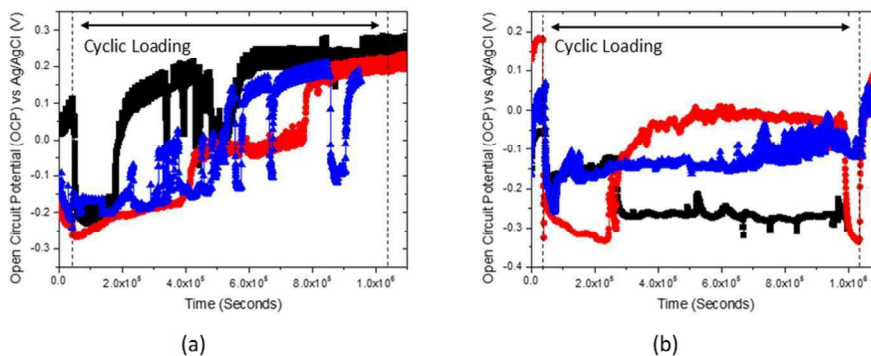
- 1  
2  
3 **15 Morlock, M., Bünthe, D., Gührs, J. and Bishop, N.** Corrosion of the Head-Stem Taper  
4 Junction—Are We on the Verge of an Epidemic? *HSS Journal*®, 2017, **13**(1), 42-49.
- 5 **16 Hothi, H.S., Matthies, A.K., Berber, R., Whittaker, R.K., Skinner, J.A. and Hart, A.J.** The  
6 Reliability of a Scoring System for Corrosion and Fretting, and Its Relationship to Material Loss of  
7 Tapered, Modular Junctions of Retrieved Hip Implants. *The Journal of Arthroplasty*, 2014, **29**(6),  
8 1313-1317.
- 9 **17 Pourzal, R., Hall, D.J., Ha, N.Q., Urban, R.M., Levine, B.R., Jacobs, J.J. and Lundberg, H.J.**  
10 Does Surface Topography Play a Role in Taper Damage in Head-neck Modular Junctions? *Clinical*  
11 *Orthopaedics and Related Research*, 2016, **474**(10), 2232-2242.
- 12 **18 Bryant, M., Farrar, R., Freeman, R., Brummitt, K. and Neville, A.** Fretting corrosion  
13 characteristics of polished collarless tapered stems in a simulated biological environment. *Tribology*  
14 *International*, 2013, **65**(0), 105-112.
- 15 **19 Panagiotidou, A., Meswania, J., Osman, K., Bolland, B., Latham, J., Skinner, J., Haddad, F.S.,**  
16 **Hart, A. and Blunn, G.** The effect of frictional torque and bending moment on corrosion at the taper  
17 interface: An in vitro study. *Bone and Joint Journal*, 2015, **97-B**(4), 463-472.
- 18 **20 Panagiotidou, A., Meswania, J., Hua, J., Muirhead-Allwood, S., Hart, A. and Blunn, G.**  
19 Enhanced wear and corrosion in modular tapers in total hip replacement is associated with the  
20 contact area and surface topography. *Journal of Orthopaedic Research*, 2013, **31**(12), 2032-2039.
- 21 **21 Bishop, N., Witt, F., Pourzal, R., Fischer, A., Rüttschi, M., Michel, M. and Morlock, M.** Wear  
22 patterns of taper connections in retrieved large diameter metal-on-metal bearings. *Journal of*  
23 *Orthopaedic Research*, 2013, **31**(7), 1116-1122.
- 24 **22 Hexter, A., Panagiotidou, A., Singh, J., Skinner, J. and Hart, A.** MECHANISM OF CORROSION  
25 IN LARGE DIAMETER HEAD METAL-ON-METAL TOTAL HIP ARTHROPLASTY: A RETIREVAL ANALYSIS OF  
26 161 COMPONENTS. *Orthopaedic Proceedings*, 2013, **95-B**(SUPP 12), 4-4.
- 27 **23 Zeng, P., Rainforth, W.M. and Cook, R.B.** Characterisation of the oxide film on the taper  
28 interface from retrieved large diameter metal on polymer modular total hip replacements. *Tribology*  
29 *International*, 2015, **89**, 86-96.
- 30 **24 Bryant, M.G., Buente, D., Oladokun, A., Ward, M., Huber, G., Morlock, M. and Neville, A.**  
31 Surface and subsurface changes as a result of tribocorrosion at the stem-neck interface of bi-  
32 modular prosthesis. *Biotribology*, 2017, **10**(Supplement C), 1-16.
- 33 **25 Bryant, M., Farrar, R., Freeman, R., Brummitt, K. and Neville, A.** The role of surface pre-  
34 treatment on the microstructure, corrosion and fretting corrosion of cemented femoral stems.  
35 *Biotribology*, 2016, **5**, 1-15.
- 36 **26 Mroczkowski, M.L., Hertzler, J.S., Humphrey, S.M., Johnson, T. and Blanchard, C.R.** Effect  
37 of impact assembly on the fretting corrosion of modular hip tapers. *Journal of Orthopaedic Research*,  
38 2006, **24**(2), 271-279.
- 39 **27 Preuss, R., Lars Haeussler, K., Flohr, M. and Streicher, R.M.** Fretting Corrosion and Trunnion  
40 Wear—Is it Also a Problem for Sleeved Ceramic Heads? *Seminars in Arthroplasty*, 2012, **23**(4), 251-  
41 257.
- 42  
43  
44  
45  
46  
47  
48  
49  
50  
51  
52  
53  
54  
55  
56  
57  
58  
59  
60



Schematic arrangement of stem orientation according to ASTM F 1875-98 a) Method I - Upright and b) Method II - Inverted.

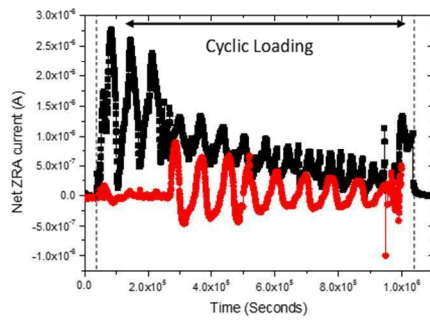
125x59mm (150 x 150 DPI)

1  
2  
3  
4  
5  
6  
7  
8  
9  
10  
11  
12  
13  
14  
15  
16  
17  
18  
19  
20  
21  
22  
23  
24  
25  
26  
27  
28  
29  
30  
31  
32  
33  
34  
35  
36  
37  
38  
39  
40  
41  
42  
43  
44  
45  
46  
47  
48  
49  
50  
51  
52  
53  
54  
55  
56  
57  
58  
59  
60

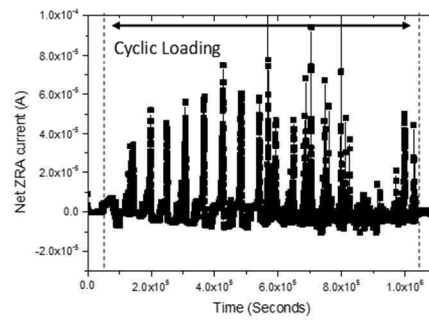


Open circuit potential measurements (OCP) for a) upright and b) mixed potential measurements for inverted stemmed components

167x73mm (150 x 150 DPI)



(a)



(b)

ZRA current measurements from Method II (Inverted) for repeat a) 1 & 3 and b) 2. Both measurements show data from the same tests. The second repeat has been plotted separately for clarity.

168x73mm (150 x 150 DPI)

1  
2  
3  
4  
5  
6  
7  
8  
9  
10  
11  
12  
13  
14  
15  
16  
17  
18  
19  
20  
21  
22  
23  
24  
25  
26  
27  
28  
29  
30  
31  
32  
33  
34  
35  
36  
37  
38  
39  
40  
41  
42  
43  
44  
45  
46  
47  
48  
49  
50  
51  
52  
53  
54  
55  
56  
57  
58  
59  
60

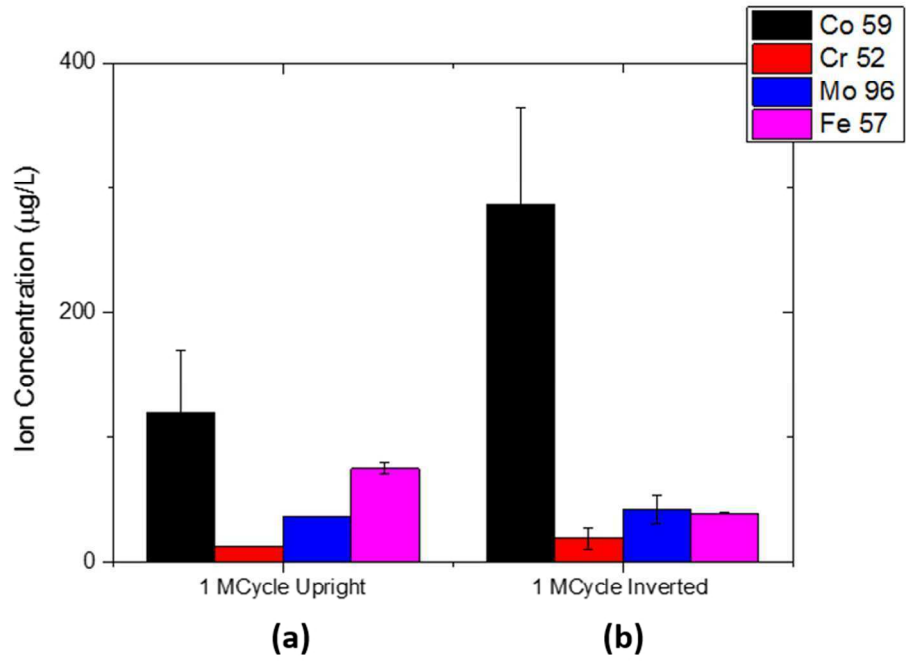


Fig 4: ICP-MS data from a) upright and b) inverted test orientation after 1 million cycles of loading.

156x110mm (150 x 150 DPI)



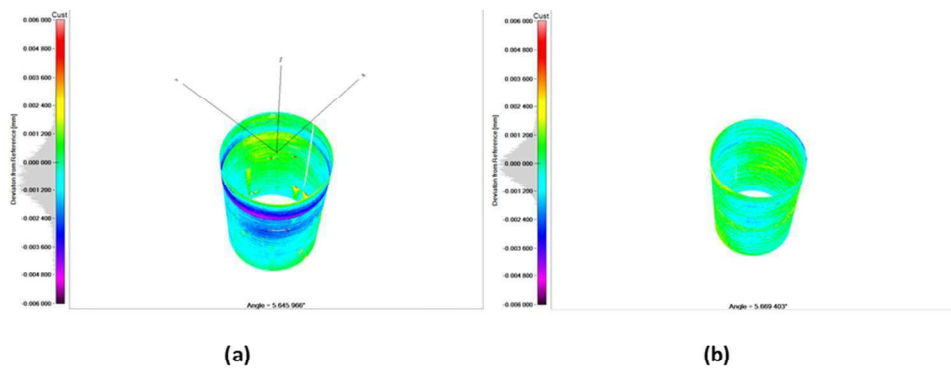
Photographs of surfaces after 1 million cycles of loading in the upright cell

159x155mm (150 x 150 DPI)

1  
2  
3  
4  
5  
6  
7  
8  
9  
10  
11  
12  
13  
14  
15  
16  
17  
18  
19  
20  
21  
22  
23  
24  
25  
26  
27  
28  
29  
30  
31  
32  
33  
34  
35  
36  
37  
38  
39  
40  
41  
42  
43  
44  
45  
46  
47  
48  
49  
50  
51  
52  
53  
54  
55  
56  
57  
58  
59  
60

	Male Trunnion	Female Taper
Inverted 1		
Inverted 2		
Inverted 3		

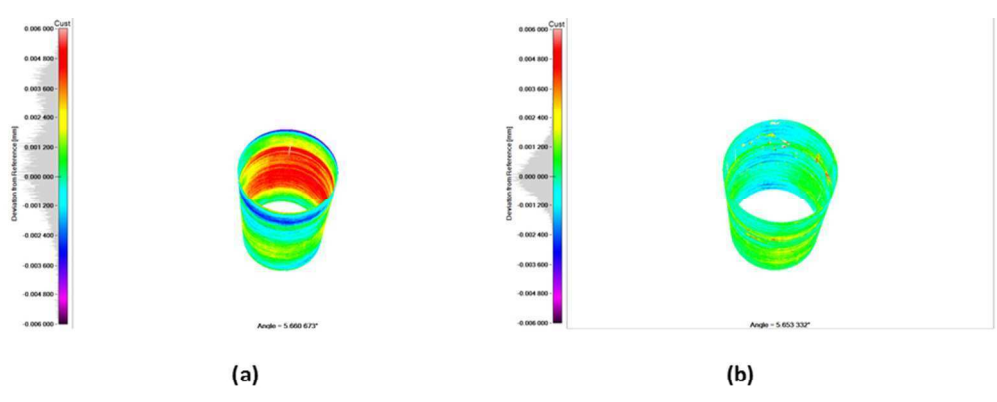
Photographs of surfaces after 1 million cycles of loading in the inverted cell  
159x159mm (150 x 150 DPI)



CMM deviation plots for the female taper of the upright cell. Note that positive deviation represents material loss. a-b represent 'upright 1' and 'upright 2' respectively (Fig 5).

165x72mm (150 x 150 DPI)

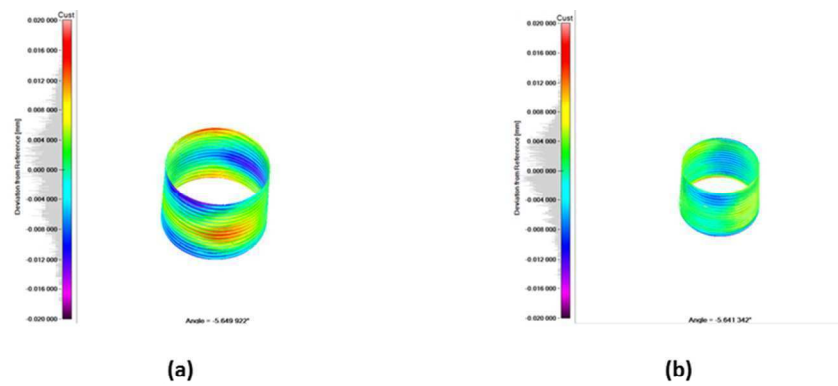
1  
2  
3  
4  
5  
6  
7  
8  
9  
10  
11  
12  
13  
14  
15  
16  
17  
18  
19  
20  
21  
22  
23  
24  
25  
26  
27  
28  
29  
30  
31  
32  
33  
34  
35  
36  
37  
38  
39  
40  
41  
42  
43  
44  
45  
46  
47  
48  
49  
50  
51  
52  
53  
54  
55  
56  
57  
58  
59  
60



CMM deviation plots for the female taper of the inverted cell. Note that positive deviation represents material loss. a-b represent 'inverted 1' and 'inverted 2' respectively (Fig 6).

160x72mm (150 x 150 DPI)

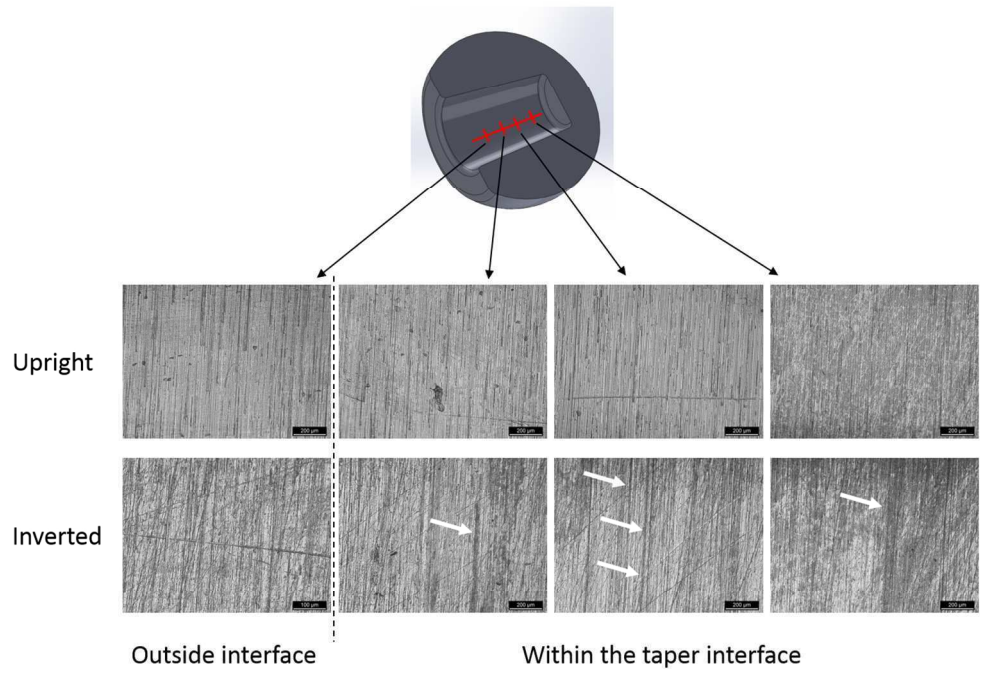
Peer Review



CMM deviation plots for the male trunnion from the a) 'upright 1' and b) 'inverted 1' after 1 million cycles of loading. Note that positive deviation represents material gain.

159x72mm (150 x 150 DPI)

1  
2  
3  
4  
5  
6  
7  
8  
9  
10  
11  
12  
13  
14  
15  
16  
17  
18  
19  
20  
21  
22  
23  
24  
25  
26  
27  
28  
29  
30  
31  
32  
33  
34  
35  
36  
37  
38  
39  
40  
41  
42  
43  
44  
45  
46  
47  
48  
49  
50  
51  
52  
53  
54  
55  
56  
57  
58  
59  
60



Optical Microscope Images of modular taper surfaces after 1 million cycles. Clear differences in the damage appearance can be seen based on device orientation. White arrows indicated evidence of trunnion thread imprinting.

240x168mm (150 x 150 DPI)

view

Experiment	Charge transfer (Q)	Estimated corrosive mass loss (mg)
Inverted 1 (Fig 3a – red)	0.03	0.01
Inverted 2 (Fig 3b)	0.74	0.23
Inverted 3 (Fig 3a – black)	0.80	0.24

Total charge transferred over 1 million cycles of loading for inverted systems

159x51mm (150 x 150 DPI)

Or Peer Review

### **LIST OF FIGURES AND TABLES**

**Fig 1:** Schematic arrangement of stem orientation according to ASTM F 1875-98 a) Method I - Upright and b) Method II - Inverted.

**Fig 2:** Open circuit potential (OCP) measurements for a) upright and b) mixed potential measurements for inverted stemmed components.

**Fig 3:** ZRA current measurements from Method II (Inverted) for repeat a) 1 & 3 and b) 2. Both measurements show data from the same tests. The second repeat has been plotted separately for clarity.

**Figure 4:** ICP-MS data from a) upright and b) inverted test orientation after 1 million cycles of loading.

**Fig 5:** Photographs of surfaces after 1 million cycles of loading in the upright cell

**Fig 6:** Photographs of surfaces after 1 million cycles of loading in the inverted cell

**Fig 7:** CMM deviation plots for the female taper of the upright cell. Note that positive deviation represents material loss. a-b represent 'upright 1' and 'upright 2' respectively (Fig 5).

**Fig 8:** CMM deviation plots for the female taper of the inverted cell. Note that positive deviation represents material loss. a-b represent 'inverted 1' and 'inverted 2' respectively (Fig 6).

**Fig 9:** CMM deviation plots for the male trunnion from the a) 'upright 1' and b) 'inverted 1' after 1 million cycles of loading. Note that positive deviation represents material gain.

**Fig 10:** Optical Microscope Images of modular taper surfaces after 1 million cycles. Clear differences in the damage appearance can be seen based on device orientation. White arrows indicated evidence of trunnion thread imprinting.

**Table 1** – Total charge transferred over 1 million cycles of loading for inverted systems